

## Excitonic transitions in lattice-matched $\text{Ga}_{1-x}\text{In}_x\text{As}/\text{InP}$ quantum wells

D. Gershoni, H. Temkin, and M. B. Panish

*AT&T Bell Laboratories, Murray Hill, New Jersey 07974*

(Received 27 June 1988)

We present a study of the excitons in quantum wells of  $\text{Ga}_{1-x}\text{In}_x\text{As}$  grown on InP substrates. Well-resolved optical transitions between confined particle states were measured by photoluminescence and photocurrent excitation. Well dimensions were varied from 10 to 200 Å, as ascertained by high-resolution transmission microscopy and x-ray diffraction. The combination of a detailed optical and structural characterization allows for a comparison with theory. Good agreement is obtained with calculations based on the effective-mass approximation which include band nonparabolicity effects and contain no adjustable parameters.

Quantum wells of  $\text{Ga}_{1-x}\text{In}_x\text{As}$  lattice matched to InP have been studied intensely in the last few years.<sup>1-7</sup> High-quality structures have become available through advances in epitaxial techniques driven by the technological importance of this material system. This system is different from  $\text{GaAs}/\text{Ga}_{1-x}\text{Al}_x\text{As}$  in two important aspects. First, the composition of the well material must be precisely controlled in order to assure lattice matching. Second, the ternary random alloy of the well gives rise to potential fluctuations with resulting inhomogeneous spectral line broadening. In addition, many of the parameters describing the bulk ternary, such as band offsets and effective masses are still being refined. Many attempts have been made to reconcile experimentally measured exciton energies, mostly the lowest electron-heavy-hole transition observed in photoluminescence, with the calculated values. In some instances, lattice mismatch strain was included on an *ad hoc* basis,<sup>3</sup> in others band offset values outside of the accepted range were used.<sup>8</sup>

In this work we report a detailed study of the optical properties of high-quality single and multiple quantum wells of  $\text{Ga}_{1-x}\text{In}_x\text{As}$  grown lattice matched on InP substrates by gas source molecular-beam epitaxy.<sup>9</sup> The optical spectroscopic techniques of low-temperature photoluminescence (PL), PL excitation (PLE), and photocurrent excitation (PCE) are employed in a complementary way to investigate the quantum wells. The well dimensions and composition were obtained by independent transmission electron microscopy and high-resolution x-ray diffraction measurements. Optical transitions, up to  $n=3$ , between single carriers confined states measured by these experiments are in very good agreement with calculations which include band nonparabolicity effects and contain no adjustable parameters. The calculation uses the best parameter values available and consistency with the binary parent values was checked where possible.

The study was done on seven quantum wells from four different samples. These consisted of a sample containing four narrow wells with thicknesses determined by transmission electron microscopy to be 9, 15, 30, and 47 Å, separated by 120-Å-thick InP barriers, and three samples with ten wells each grown as the intrinsic layer of a *p-i-n* structure. The wells of the multi-quantum-well samples were 79, 142, and 189 Å thick. For the measure-

ment of the PCE spectra, 100- $\mu\text{m}$ -diameter mesa-type diodes were fabricated from these wafers. All the samples were grown at 500°C on (100)-oriented InP substrates using previously described procedures.<sup>10</sup> The residual  $n$ -type doping level of  $\text{Ga}_{0.47}\text{In}_{0.53}\text{As}$  was in the range of  $(0.5-1) \times 10^{16} \text{ cm}^{-3}$ .

The low-temperature ( $\sim 10 \text{ K}$ ) PL and PLE spectra of the four-layer quantum-well sample are shown in Fig. 1. The PLE experiments were carried out using tungsten lamp light dispersed through a 0.64-m spectrometer as a continuous excitation source. The PL spectrum of the sample, obtained here using the lamp source at above InP band-gap excitation is shown in the lower trace of Fig. 1. It is dominated by lines due to the excitonic recombination of electrons and heavy holes from the  $n=1$  subband levels (1H). The lines are intense and quite narrow, as discussed previously.<sup>10</sup> Quantum size effects commensurate with the narrow wells result in the large exciton energy shifts, close to the band gap of InP. The PLE spectra of individual quantum wells are shown displaced one above the other. Excellent luminescence efficiency of the material allows us to observe the PLE spectrum even from a 9-Å-thick well. In addition to the 1H exciton transition,

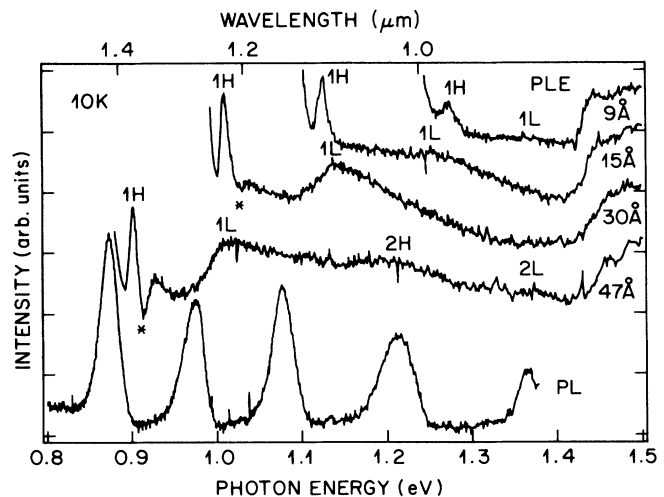


FIG. 1. Low-temperature PL and PLE spectra of a four  $\text{Ga}_{1-x}\text{In}_x\text{As}$  quantum wells sample.

all the wells also show well-resolved electron-to-light-hole exciton transitions ( $1L$ ). However,  $1L$  peak of the narrowest well is quite broad and weak. The  $1H$  exciton transition energies measured by PLE are all at higher energies than the PL peaks and the relative blue shift of the PLE peaks becomes greater in narrower wells. At 9 meV above the  $1H$  exciton of the 47-Å-wide well we observe a dip in the PLE response. A similar, but weaker dip is observed in the 30-Å well PLE spectrum. We interpret these features as the onset of the continuum for a hydrogenlike two-dimensional (2D) heavy-hole exciton. Following Miller, Kleinman, Tsang, and Gossard,<sup>11</sup> an exciton binding energy of  $\sim 10$  meV is obtained from this shift.

The spectra obtained on a ternary structure consisting of 10  $\text{Ga}_{1-x}\text{In}_x\text{As}$  wells, each 79 Å thick, separated by 460-Å InP layers are shown in Fig. 2. Their dimensions were determined to within a monolayer using high-resolution x-ray diffraction, as discussed before.<sup>12</sup> The quantum wells were confined within the intrinsic layer of a  $p-i-n$  structure. This has allowed us to study the PL, PLE, and photocurrent excitation (PCE) spectra as a function of bias on the same sample. Its PL spectrum is also dominated by a single line at 0.843 eV which is due to the excitonic recombination of electron and heavy hole from the  $n=1$  subband level ( $1H$ ). Another line, with the intensity lower by at least three orders of magnitude, is seen 63 meV higher in energy. This line is due to recombination of the  $n=1$  electron-light-hole exciton ( $1L$ ). The intensity ratio between the two luminescence lines reflects the ratio of the radiative lifetime of the carriers, to the thermalization time of holes to their lowest-energy state. Consequently, from the known former value [approximately 2 nsec (Refs. 13 and 14)] one can estimate the later to be of the order of 1 psec. The additional PL features, a broad line between 1.1 and 1.2 eV and a triplet of sharp lines at 1.373, 1.335, and 1.297 eV originate in InP. The broad line is probably one of many spectral features observed in this region and associated with com-

plexes of native defects and transition-metal impurities.<sup>15,16</sup> The three high-energy lines are due to donor-acceptor (Be) pairs and their two LO-phonon replica.<sup>17</sup> The PLE spectrum shows very well resolved lines due to  $1H$ ,  $1L$ ,  $2H$ , and  $2L$  transitions at energies of 0.858, 0.905, 1.028, and 1.134 eV, respectively. These peaks are also observed in the PCE spectrum which was taken under a slight forward bias in order to eliminate Stark shifts of the exciton peaks (at helium temperatures photocarrier emission from the well is inhibited at zero bias). The  $1H$  line in the PL spectrum is again red shifted, this time by as much as 15 meV, from the transition energy measured in the PLE and PCE experiments. In contrast, the  $1L$  line does not exhibit any shift. We argue that the red shift of the  $1H$  PL peak is due to recombination processes which involve excitons bound to potential fluctuations in the quantum well. These may arise either from composition fluctuations or, less likely, interface roughness. At low temperatures, excitons are rapidly thermalized to localized states of lower energy associated with these potential fluctuations. The absence of such a red shift in the  $1L$  transition indicates that the time for exciton thermalization to a state associated with the potential fluctuation is longer than the hole thermalization time to the lowest-energy state. This is in good agreement with recently measured localized exciton hopping time of 16 psec.<sup>14</sup> Radiative recombination of the  $1H$  excitons bound to those final states gives rise both to the observed red shift and to the narrower PL linewidth (11 meV) compared to the width of the same line measured in absorption (14 meV). The linewidth obtained in absorption measurements is more indicative of the intrinsic density of the exciton states and it should be used to characterize the sample quality.<sup>18</sup> The blue shift of the PLE peaks becomes greater in narrower wells. This resembles the behavior of excitons bound to impurities in quantum wells, as was previously seen by Miller, Gossard, Tsang, and Munteana in GaAs wells<sup>19</sup> and calculated by Bastard.<sup>20</sup> The exciton binding to potential fluctuations is expected to produce a similar red shift. The shift may be even more sensitive to the well

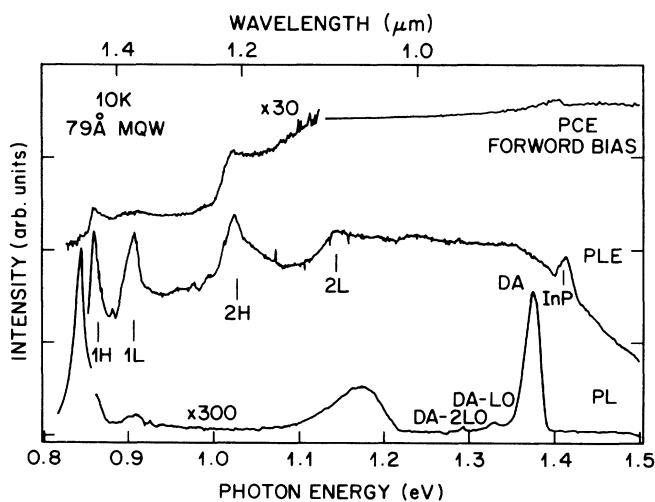


FIG. 2. Low-temperature PL, PLE, and PCE spectra of a 10-well sample. Quantum wells are forming the intrinsic region of a  $p-i-n$  structure.

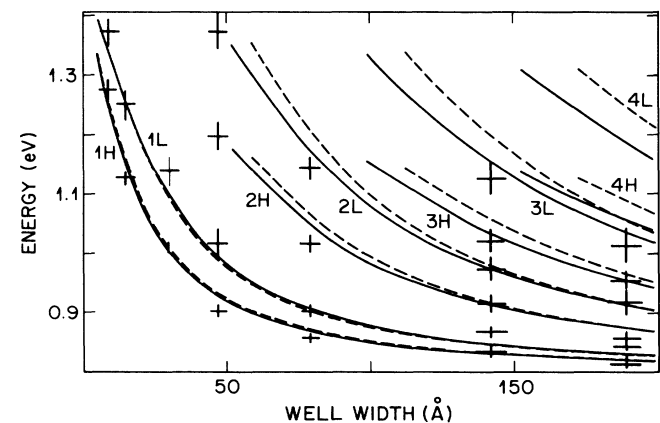


FIG. 3. Exciton transition energies as a function of the quantum-well width. Points represent experimental data obtained by PLE, bars represent the experimental uncertainties. Solid (dashed) lines show the calculated transition energies, including (neglecting) nonparabolicity effects.

TABLE I. Constants used in calculations.

Name	InP	GaAs	InAs	Ga <sub>0.47</sub> In <sub>0.53</sub> As
$E_g$ (eV)	1.424 <sup>a</sup>	1.519 <sup>a</sup>	0.418 <sup>a</sup>	0.812 <sup>b</sup>
$\Delta_{so}$ (eV)	0.11 <sup>a</sup>	0.34 <sup>a</sup>	0.37 <sup>a</sup>	0.356 <sup>c</sup>
$m^e$ (emu)	0.079 <sup>a</sup>	0.067 <sup>a</sup>	0.023 <sup>a</sup>	0.041 <sup>c,d</sup>
$m_z^{lh}$ (emu)	0.121 <sup>e</sup>	0.094 <sup>f</sup>	0.027 <sup>e</sup>	0.056 <sup>c,d</sup>
$m_z^{hh}$ (emu)	0.606 <sup>e</sup>	0.341 <sup>e,f</sup>	0.4 <sup>e</sup>	0.377 <sup>c,d</sup>
Valence-band offset (eV) relative to InP	0	0.34 <sup>g</sup>	0.41 <sup>g</sup>	0.37 <sup>c,h</sup>

<sup>a</sup>*Semiconductors*, edited by O. Madelung, M. Schulz, and H. Weiss, Landolt-Börnstein, New Series, Group 3, Vol. 17a (Springer, Berlin, 1982).

<sup>b</sup>*GaInAsP Alloy Semiconductors*, edited by T. P. Pearsall (Wiley, New York, 1982).

<sup>c</sup>Linearly interpolated from the binary materials data.

<sup>d</sup>K. Alavi and R. L. Aggrawal, Phys. Rev. B **21**, 1311 (1980), in very close agreement with footnote c

<sup>e</sup>We use  $m_z^{lh} = 1/(\gamma_1 + 2\gamma_2)m_z^{hh} = 1/(\gamma_1 - 2\gamma_2)$  and Luttinger parameters  $\gamma_1, \gamma_2$  from footnote a.

<sup>f</sup>D. F. Nelson, R. C. Miller, and D. A. Kleinman, Phys. Rev. B **35**, 7770 (1987).

<sup>g</sup>R. S. Bauer and G. Margaritondo, Phys. Today **40** (No. 1), 27 (1987).

<sup>h</sup>S. R. Forrest, P. H. Schmidt, R. B. Wilson, and M. L. Kaplan, Appl. Phys. Lett. **45**, 1199 (1984).

dimensions than the case of the exciton bound to impurities. This is because the exciton radius decreases with the quantum well width and this in turn reduces the volume it samples. The average over a smaller volume results in deeper potential fluctuations and thus a larger binding energy. As discussed below, the 1H and 1L energies measured by PLE are in good agreement, in contrast with those measured by PL, with the calculated values.

The optical transition energies measured at low temperatures by absorption techniques in the samples discussed above, together with the data obtained on two other samples with wider quantum wells (142 and 189 Å), are plotted in Fig. 3 as a function of quantum well width. The confined carriers' energies were calculated by numerically finding the root of the following equation:

$$f(E) = [r_1(E) - 1/r_1(E)]\sin r_2(E) - 2\cos r_2(E), \quad (1)$$

where  $r_1(E) = k_w(E)m_b(E)/k_b(E)m_w(E)$  and  $r_2(E) = k_w(E)L_w$ ;  $L, k, m$  stand for the width, carrier wave vectors, and effective masses in the confinement direction, and the subscripts  $w$  and  $b$  denote the well and barrier, respectively. The dispersion relations which correlate the wave vector to the particle energy  $E$  are then

$$E = \hbar^2 k_w^2 / 2m_w(E), \quad E - V_b = \hbar^2 k_b^2 / 2m_b(E), \quad (2)$$

where  $V_b$  is the barrier potential, or band discontinuity. The effects of band nonparabolicity were introduced through the energy-dependent effective masses of electrons and light holes:

$$m(E) = \hbar^2 k^2(E) / 2E, \quad (3)$$

where  $k(E)$  is given implicitly by the Kane-model dispersion relation<sup>21</sup>

$$(E')(E' - E_g)(E' + \Delta_{so}) - k^2 P^2 (E' + 2\Delta_{so}) = 0. \quad (4)$$

Here  $E' = E + E_B - \hbar^2 k^2 / 2m_0$ , where  $E_B$  is the relevant band energy, i.e.,  $E_g(0)$  for electron (light-hole),  $E_g$  and  $\Delta_{so}$  the material band gap and split-off energies, and  $P$  is the  $k \cdot p$  matrix element. The last was chosen so that  $m(E=0)$  is given by the known band-edge effective masses listed in Table I. (Different  $P$  values are used for electron and light hole.<sup>22</sup>) In the barriers the energy  $E$  is replaced by  $E - V_b$ . Thus the nonparabolicity is calculated from the  $k \cdot p$  theory and is not a free parameter. The dashed lines in Fig. 3 represent transition energies calculated neglecting the nonparabolicity effects. These are included in the calculation represented by the solid lines. The inclusion of nonparabolicity has a negligible effect on the calculated energy of the lowest-order excitonic transitions. However, a considerable effect is seen in the higher-order transitions. For these the inclusion of nonparabolicity results in a better agreement with the data. The calculation also includes the exciton binding energy as estimated above. However, other small effects, such as the background doping in the wells (Moss-Burstein shift) and the binding-energy size dependence are neglected. From an experimental point of view these corrections are at most comparable to the intrinsic linewidth of optical transitions in this material system.

In summary, a detailed comparison between the measured and calculated excitonic transitions in lattice matched wells of Ga<sub>1-x</sub>In<sub>x</sub>As/InP is presented. The well dimensions were varied over a wide range and their thicknesses independently measured. Well resolved optical transitions, up to  $n=3$ , have been observed by absorption and photoluminescence techniques. The exciton binding energy for a  $\sim 50$ -Å quantum well, and hole thermalization time, have been deduced from these measurements. Very good agreement has been obtained with calculations which include band nonparabolicity effects calculated from the four-band  $k \cdot p$  theory. The calculation used the best parameter values available and we have assured their consistency with the binary parent values.

- <sup>1</sup>M. Razeghi, S. P. Hirtz, U. O. Ziemelis, C. Delaude, R. Etienne, and M. Voos, *Appl. Phys. Lett.* **43**, 585 (1983).
- <sup>2</sup>H. Temkin, M. B. Panish, P. M. Petroff, R. A. Hamm, J. M. Vandenberg, and S. Samski, *Appl. Phys. Lett.* **47**, 394 (1985).
- <sup>3</sup>M. S. Skolnick, L. L. Taylor, S. J. Bass, A. D. Pitt, D. J. Mowbrag, A. G. Cullis, and N. G. Chew, *Appl. Phys. Lett.* **51**, 29 (1987).
- <sup>4</sup>C. P. Kuo, K. L. Fry, and G. B. Stringfellow, *Appl. Phys. Lett.* **42**, 855 (1985).
- <sup>5</sup>B. I. Miller, E. F. Schubert, U. Koren, A. Ourmazd, A. H. Dayeln, and R. J. Capik, *Appl. Phys. Lett.* **49**, 1384 (1987).
- <sup>6</sup>W. T. Tsang and E. F. Schubert, *Appl. Phys. Lett.* **49**, 220 (1986).
- <sup>7</sup>Yoshihiro Kawagachi and Hajime Asahi, *Appl. Phys. Lett.* **50**, 1243 (1987).
- <sup>8</sup>R. Sauer, T. D. Harris, and W. T. Tsang, *Phys. Rev. B* **34**, 9023 (1986).
- <sup>9</sup>M. B. Panish, H. Temkin, and S. Samski, *J. Vac. Sci. Technol. B* **3**, 657 (1985).
- <sup>10</sup>M. B. Panish, H. Temkin, R. A. Hamm, and S. N. G. Chu, *Appl. Phys. Lett.* **49**, 164 (1986).
- <sup>11</sup>R. C. Miller, D. A. Kleinman, W. T. Tsang, and A. C. Gosard, *Phys. Rev. B* **24**, 1134 (1981).
- <sup>12</sup>D. Gershoni, J. M. Vanderberg, R. A. Hamm, H. Temkin, and M. B. Panish, *Phys. Rev. B* **36**, 1320 (1987).
- <sup>13</sup>J. Feldman, G. Peter, E. O. Gobel, P. Dawson, K. Moore, C. Foxon, and R. J. Elliott, *Phys. Rev. Lett.* **59**, 2337 (1987).
- <sup>14</sup>J. Hegarty, K. Tai, and W. T. Tsang, this issue, *Phys. Rev. B* **38**, 7843 (1988).
- <sup>15</sup>H. Temkin, B. V. Dutt, and W. A. Bonner, *Appl. Phys. Lett.* **38**, 431 (1981).
- <sup>16</sup>A. M. Loshinskii, E. M. Omel'yanovskii, and A. Ya. Polyakov, *Fiz. Tekh. Poluprovodn.* **19**, 1986 (1985) [*Sov. Phys. Semicond.* **19**, 1223 (1985)].
- <sup>17</sup>E. Kubota and A. Katsui, *J. Appl. Phys.* **59**, 3841 (1986).
- <sup>18</sup>R. C. Miller and R. Bhat, *J. Appl. Phys.* (to be published).
- <sup>19</sup>R. C. Miller, A. C. Gosard, W. T. Tsang, and O. Munteana, *Phys. Rev. B* **25**, 3871 (1982).
- <sup>20</sup>G. Bastard, *Phys. Rev. B* **24**, 4714 (1981).
- <sup>21</sup>E. O. Kane, *J. Phys. Chem. Solids* **1**, 249 (1957).
- <sup>22</sup>J. S. Blakemore, *J. Appl. Phys.* **53**, R123 (1982).